



Original Research Article

A STANDARD DEVIATION CONTROL CHART FOR MARSHALL–OLKIN ALPHA POWER INVERSE RAYLEIGH DISTRIBUTION

Ismaila Olawale Adegbite^{1*}, Kayode Samuel Adekeye², Semiu Ayinla Alayande¹ and Odunayo Adiat Oyegoke¹

¹ Department of Mathematics and Statistics, Redeemer's University, Ede, Osun State, Nigeria

² DVC (T&L) Office, University of The Gambia, MDI Road, Kanifing, The Gambia

All correspondence should be addressed to Olawale Adegbite: adegbiteonline@gmail.com

ABSTRACT

The conventional SPC charts, including the Shewhart standard deviation chart, are prone to failure due to skewed or heavy-tailed data, resulting in false alarms and an inability to detect shifts in variability. The primary objective of this study is to develop a deviation control chart based on percentiles of the Marshall-Olkin Alpha Power Inverse Rayleigh Distribution (MOAPIRD) of non-normal processes. Empirical MOAPIRD percentiles are used to derive the control limits giving correct probability limits. The simulations of different parameters and sample sizes demonstrate that MOAPIRD chart can have a large average run length (ARL) and very low standard deviation of run length (SDRL) in most scenarios, it outperforms other techniques like the Shewhart and Inverse Rayleigh distribution charts. The chart is validated against real engine oil viscosity data which confirms the reliability of the chart which effectively accommodates skewness and heavy tails without spurious uncontrolled signals. The chart based on MOAPIRD is suggested when it is necessary to accurately monitor the variability of the processes in the unusual industrial settings.

Keywords: Control Chart, Dispersion, MOAPIRD, Skewness, Statistical Process Control, Standard Deviation.

1.0 INTRODUCTION

Statistical Process Control (SPC) provides a valuable framework of monitoring, analyzing and enhancing process quality in industry and service organizations. Control charts are the most potent SPC tools to differentiate between random cause and assignable cause variation and therefore assisting the organizations to ensure stability of the quality of their products and identify deviations at an earlier stage (Chou et al., 2001). One of the most common tools that are used when evaluating the variability of processes is the Shewhart standard deviation (S) control chart. Nonetheless, its accuracy is also based on the fact that the quality feature must take a normal distribution, a condition that is hardly realistic in practical scenarios (Chang and Bai, 2001; Chan and Cui, 2003). Normal-theory control charts are prone to false alarms and loss of sensitivity to real shifts in the process, since in most manufacturing and health-care processes data are skewed or heavy-tailed (Chen, 1996).

To address these shortcomings, scholars have proposed quite a number of approaches to help control-chart to improve performance in non-normal situations. Chang and Bai (2001) designed the population charts of positively skewed standard deviations whereas Chan and Cui (2003)

designed skewness-correction (SC) charts to track the asymmetric processes. To derive robust limits of non-normal data, Adekeye and Azubuike (2012) used the Median Absolute Deviation (MAD), and Shibo et al. (2014) developed a Weighted Standard Deviation (WSD) chart. Atta et al. (2020) subsequently suggested an SC-S chart and a scaled-WSD-based R chart where the population is skewed. Subsequent scholars like Aako et al. (2020), Adewara et al. (2020), Ying-Chin et al. (2021), Wan and Zhu (2022), and Aako et al. (2024) have continued to develop dispersion-chart design in terms of positively skewed distributions, showing that non-normal data require specialized analytical.

Similar research has highlighted the impracticability of normal-theory charts. Improper use of normal-based limits may cause undue Type I and II errors, unwarranted changes, and the production of non-conforming items at a substantially high price (Montgomery, 2013). As a result of this, more recent SPC studies have been focused on more adaptive models - data transformations, robust estimators, and, more importantly, distribution-specific control charts that incorporate the underlying probability model into chart construction. Examples include charts based on Exponentiated Lomax (Adewara and Ako, 2018), Gompertz (Adewara et al., 2020), New Rayleigh -Pareto (Rosaiah et al., 2021) and Generalized lognormal (Panda & Wang, 2025) distribution charts. Oladipupo et al. (2025) improved the Non-parametric Double Homogeneously Weighted Moving Average (NPIRDHWMA) control chart to monitor changes in the process location..

Based on these developments, Malik and Ahmad (2018) suggested the Alpha Power Inverse Rayleigh Distribution (APIRD), an integration of Inverse Rayleigh model with alpha-power transformation to fit an inflexible positively skewed data. In order to enhance flexibility with heavy-tailed industry data, Adegbite et al. (2024) subsequently studied and used the Marshall-Olkin generalization to obtain the Marshall-Olkin Alpha Power Inverse Rayleigh Distribution (MOAPIRD). This additional parameter is remarkable in adding to the model the capability to capture any number of skewness and tail properties of distribution. This paper presents a control chart of standard deviation (S) that is designed based on percentiles of MOAPIRD framework to control variability in processes of skewed datasets situations. The proposed chart control limits are determined based on the variance percentiles calculated with the help of the MOAPIRD methodology, which will guarantee the proper control of false alarms and increased sensitivity to variations in true variability. Simulated and real-process data are used to do comparative analyses against Shewhart, Inverse Rayleigh distribution (IRD) based charts, which are used to justify its practical superiority.

2.0 THE MARSHALL-OLKIN ALPHA POWER INVERSE RAYLEIGH DISTRIBUTION (MOAPIRD)

The probability density function (pdf), the cumulative distribution function (cdf), and the survival function of MOAPIRD, as described by Adegbite et al. (2024), are

$$g_{MOAPIR}(x; \alpha, \lambda, \theta) = \begin{cases} \frac{(\alpha-1)2\lambda\theta \log(\alpha)x^{-3}e^{-\lambda x^{-2}}\alpha^{e^{-\lambda x^{-2}}}}{[(\alpha-1)\theta+(1-\theta)(\alpha^{e^{-\lambda x^{-2}}}-1)]^2} & x > 0, \alpha \neq 1, \lambda > 0, \theta > 0 \\ 0, & \alpha = 1 \end{cases} \quad (1)$$

$$G_{MOAPIR}(x; \alpha, \lambda, \theta) = \begin{cases} \frac{\alpha^{e^{-\lambda x^{-2}}} - 1}{\theta(\alpha-1) + (1-\theta)(\alpha^{e^{-\lambda x^{-2}}} - 1)}, & x > 0, \alpha \neq 1, \lambda > 0, \theta > 0 \\ 0 & \alpha = 1 \end{cases} \quad (2)$$

The survival function is

$$R_{MOAPIR}(x) = \begin{cases} \frac{\alpha\theta(1-\alpha^{e^{-\lambda x^{-2}}}-1)}{\theta(\alpha-1)+(1-\theta)(\alpha^{e^{-\lambda x^{-2}}}-1)}, & x > 0, \alpha \neq 1, \lambda > 0, \theta > 0 \\ 0 & \alpha = 1 \end{cases} \quad (3)$$

, where α , λ , and θ are shape, scale, and location parameters, respectively.

2.1 Proposed Standard Deviation Chart Based on Percentiles of MOAPIRD

The control limits of the sample standard deviation (s) have a probability limit of 0.9973 in MOAPIRD. This implies that lower and upper control limits will assume the following form:

$$P(L \leq s \leq U) = 0.9973 \quad (4)$$

$s = \sqrt{V(x)}$ (5)
 , where $V(x)$ is defined by Adegbite et al. (2024) as

$$V(X) = \sum_{k=0}^{\infty} \sum_{j=0}^k \sum_{m=0}^{\infty} W_{k,j,m}((m+1)\lambda) - \left(\Gamma\left(\frac{1}{2}\right) \sum_{k=0}^{\infty} \sum_{j=0}^k \sum_{m=0}^{\infty} W_{k,j,m}((m+1)\lambda)^{\frac{1}{2}} \right)^2 \quad (6)$$

, where

$$W_{k,j,m} = \begin{cases} (-1)^j \binom{k}{j} (k+1) \frac{(\theta-1)^k (k-j+1)^m (\log(\alpha))^{m+1}}{\theta^{k+1} (\alpha-1)^{k+1} (m+1)!}, & \theta > 1 \\ (-1)^j \binom{k}{j} (k+1) \frac{(1-\theta)^k (j+1)^m (\log(\alpha))^{m+1}}{\theta^{k+1} (\alpha-1)^{k+1} (m+1)!}, & 0 < \theta < 1 \end{cases} \quad (7)$$

Using the equal-tailed approach, L and U are equal to the 0.00135th and 0.99865th percentiles of the standard deviation sampling distribution, respectively. But in the case of MOAPIRD distribution, the standard deviation

of the sampling distribution cannot be calculated mathematically. As such, we employed the use of the simulation method to determine the empirical standard deviation sampling distribution and determine its percentiles. The sample standard deviation control limits in MOAPIRD are set at the probability level of 0.9973, such that the samples assume the following form:

$$P(Z_{0.00135} \leq s \leq Z_{0.99865}) = 0.9973 \quad (8)$$

The standard deviation of the sampling distribution, when 's' is the standard deviation from MOAPIRD, is characterized by parameters $\alpha = 0.5, \lambda = 3.0, \theta = 2.1; \alpha = 1.2, \lambda = 2.2, \theta = 0.4; \alpha = 1.6, \lambda = 0.2, \theta = 3.4$ and $\alpha = 1.8, \lambda = 0.5, \theta = 1.5$, corresponding to the shape, scale, and location parameters, respectively. From equation (8), for the i^{th} subgroup standard deviation, where \bar{s} is the grand mean of standard deviations and s_i is the i^{th} subgroup standard deviation is

$$P\left(Z_{0.00135} \frac{\bar{s}}{s} \leq s_i \leq Z_{0.99865} \frac{\bar{s}}{s}\right) = 0.9973 \quad (9)$$

, this can be written as,

$$P(B^*_{3p} \times \bar{s} \leq s_i \leq B^{**}_{3p} \times \bar{s}) = 0.9973 \quad (10)$$

, where $B^*_{3p} = \frac{Z_{0.00135}}{s}$, $B^{**}_{3p} = \frac{Z_{0.99865}}{s}$, \bar{s} is the grand mean of standard deviations and s_i is the i^{th} subgroup standard deviation. Thus, B^*_{3p}, B^{**}_{3p} are the constants of the s-chart for the MOAPIRD process data.

2.2. Performance Evaluation

Three indicators are utilized to assess the performance of the proposed control charts: the Control Limit Interval (CLI), the average number of samples per control, which is the Average Run Length (ARL); the

Standard Deviation of Run Length (SDRL), which is the standard deviation of the number of samples needed to produce a signal. Abu-Shawiesh et al (2020) provide the formulae of the calculation of these indicators.

3.0 RESULT AND DISCUSSION

3.1 Simulation Study

Nine data sets were simulated and arranged in 2,3,4,5,6,7,8,9, and 10 sample sizes with 30 subgroups using the Marshall-Olkin Alpha Power Inverse Rayleigh Distribution with parameters: $\alpha = 0.5, \lambda = 3.0, \theta = 2.1$; $\alpha = 1.2, \lambda = 2.2, \theta = 0.4$; $\alpha = 1.6, \lambda = 0.2, \theta = 3.1$, and $\alpha = 1.8, \lambda = 0.5, \theta = 1.5$. The control limits of the

proposed charts for different sample sizes with 30 subgroups were computed using the R programming language. The Average Run Length (ARL), Control Limit Interval (CLI), and Standard Deviation of Run Length (SDRL) of the proposed charts were also evaluated. These were compared with the existing control chart in the literature. The results of different proposed methods are presented in Table 6.

Tables 1-4 show the result of the percentiles for different levels of parameters based on the standard deviation of MOAPIRD, while Table 5 shows the percentile constants for various parameter sets.

Table 1: Percentiles at $\alpha = 0.5, \lambda = 3.0, \theta = 2.1$

n	0.99865	0.995	0.99	0.975	0.95	0.05	0.025	0.01	0.005	0.00135
2	26.8903	13.9471	9.8374	6.1745	4.3098	0.2317	0.0647	0.1093	0.0827	0.0536
3	41.6323	21.5934	15.2306	9.5597	6.6728	0.3635	0.1110	0.1777	0.1379	0.0944
4	43.0846	22.3483	15.7647	9.8981	6.9128	0.4751	0.2493	0.3129	0.2763	0.2307
5	46.3733	24.0567	16.9722	10.6610	7.4513	0.6116	0.3664	0.4404	0.3986	0.3434
6	44.9607	23.3278	16.4618	10.3475	7.2409	0.6468	0.3664	0.4523	0.4035	0.3402
7	47.2838	24.5420	17.3273	10.9080	7.6526	0.8129	0.4706	0.5802	0.5183	0.4368
8	49.7250	25.8106	18.2243	11.4754	8.0539	0.8716	0.5147	0.6285	0.5644	0.4794
9	50.0929	26.0046	18.3642	11.5690	8.1260	0.9129	0.5580	0.6712	0.6076	0.5224
10	55.9229	29.0239	20.4895	12.8948	9.0418	0.9784	0.6381	0.7475	0.6866	0.6026

Table 2: Percentiles at $\alpha = 1.2, \lambda = 2.2, \theta = 0.4$

n	0.99865	0.995	0.99	0.975	0.95	0.05	0.025	0.01	0.005	0.00135
2	12.6881	6.5809	4.6417	2.9134	2.0336	0.1095	0.0311	0.0520	0.0395	0.0259
3	19.6807	10.2078	7.1999	4.5191	3.1544	0.1718	0.0524	0.0839	0.0651	0.0445
4	20.3663	10.5642	7.4520	4.6789	3.2677	0.2245	0.1178	0.1478	0.1305	0.1090
5	21.8897	11.3555	8.0115	5.0324	3.5174	0.2896	0.1738	0.2088	0.1891	0.1629
6	21.2081	11.0039	7.7652	4.8812	3.4159	0.3065	0.1738	0.2145	0.1914	0.1615
7	22.1952	11.5205	8.1342	5.1215	3.5939	0.3872	0.2235	0.2762	0.2465	0.2072
8	23.3805	12.1364	8.5695	5.3966	3.7882	0.4139	0.2423	0.2973	0.2663	0.2253
9	23.5777	12.2400	8.6440	5.4460	3.8257	0.4323	0.2655	0.3188	0.2889	0.2487
10	26.9640	13.9920	9.8755	6.2109	4.3503	0.4635	0.3099	0.3598	0.3321	0.2934

Table 3: Percentiles at $\alpha=1.6, \lambda=0.2, \theta=3.1$

n	0.99865	0.995	0.99	0.975	0.95	0.05	0.025	0.01	0.005	0.00135
2	10.1956	5.2881	3.7299	2.3411	1.6341	0.0881	0.0250	0.0418	0.0318	0.0208
3	15.8159	8.2032	5.7860	3.6317	2.5350	0.1394	0.0447	0.0696	0.0547	0.0385
4	16.2464	8.4272	5.9447	3.7326	2.6071	0.1835	0.0985	0.1226	0.1088	0.0913
5	17.6225	9.1418	6.4495	4.0511	2.8312	0.2294	0.1364	0.1643	0.1485	0.1277
6	17.2191	8.9338	6.3040	3.9620	2.7718	0.2422	0.1367	0.1688	0.1505	0.1269
7	18.2822	9.4884	6.6982	4.2153	2.9555	0.3039	0.1745	0.2157	0.1925	0.1619
8	19.3410	10.0382	7.0867	4.4603	3.1280	0.3257	0.1938	0.2354	0.2119	0.1808
9	19.8791	10.3173	7.2837	4.5841	3.2147	0.3413	0.2165	0.2561	0.2339	0.2037
10	22.2714	11.5563	8.1558	5.1281	3.5904	0.3660	0.2406	0.2809	0.2585	0.2275

Table 4: Percentiles at $\alpha=1.8, \lambda=0.5, \theta=1.5$

n	0.99865	0.995	0.99	0.975	0.95	0.05	0.0025	0.01	0.005	0.00135
2	12.0047	6.2264	4.3917	2.7565	1.9241	0.1039	0.0299	0.0496	0.0378	0.0250
3	18.7261	9.7126	6.8507	4.2999	3.0014	0.1636	0.0503	0.0801	0.0623	0.0429
4	19.4003	10.0630	7.0985	4.4569	3.1127	0.2132	0.1115	0.1401	0.1236	0.1031
5	21.0033	10.8956	7.6868	4.8281	3.3742	0.2718	0.1611	0.1943	0.1755	0.1508
6	20.5576	10.6657	7.5259	4.7295	3.3083	0.2852	0.1617	0.1992	0.1779	0.1504
7	21.7477	11.2869	7.9678	5.0142	3.5156	0.3612	0.2064	0.2558	0.2279	0.1912
8	22.9311	11.9016	8.4023	5.2886	3.7092	0.3877	0.2254	0.2770	0.2479	0.2095
9	23.2545	12.0704	8.5224	5.3659	3.7655	0.4050	0.2441	0.2951	0.2664	0.2281
10	26.1024	13.5452	9.5604	6.0131	4.2122	0.4351	0.2833	0.3319	0.3048	0.2675

Table 5: Percentile constants of the standard deviation chart

n	$(\alpha=0.5, \lambda=3.0, \theta=2.1)$		$(\alpha=1.2, \lambda=2.2, \theta=0.4)$		$(\alpha=1.6, \lambda=0.2, \theta=3.1)$		$(\alpha=1.8, \lambda=0.5, \theta=1.5)$	
	B^*_{3p}	B^{**}_{3p}	B^*_{3p}	B^{**}_{3p}	B^*_{3p}	B^{**}_{3p}	B^*_{3p}	B^{**}_{3p}
2	0.0222	11.1257	0.0227	11.1379	0.0218	10.7227	0.0225	10.7822
3	0.034	14.9749	0.034	15.0198	0.0352	14.4638	0.0335	14.6162
4	0.0876	16.358	0.0878	16.4026	0.0885	15.7459	0.0851	16.0147
5	0.1295	17.4921	0.1303	17.5113	0.1234	17.03	0.1239	17.254
6	0.1335	17.6433	0.1344	17.6498	0.1276	17.3169	0.1285	17.5744
7	0.1589	17.2013	0.1599	17.1267	0.1507	17.0174	0.1513	17.2118
8	0.1616	16.7604	0.1611	16.7212	0.1552	16.5989	0.1532	16.7688
9	0.1764	16.9187	0.1783	16.8963	0.1753	17.1039	0.1672	17.0427
10	0.1813	16.8233	0.1874	17.2173	0.1732	16.957	0.174	16.9835

Table 5 presents Percentile Constants for a Standard Deviation Control Chart designed to monitor process, whose data follow a MOAPIRD, not the standard normal distribution. The constants B^*_{3p} and B^{**}_{3p} are used to calculate the control limits for the sample standard deviation chart for different sample sizes (n) and various underlying MOAPIRD distribution shapes. The key takeaway is that the standard control chart constants (like B_3 and B_4) are inappropriate here. The

correct constants depend heavily on the sample size (n) and the specific skewness and shape of process data, which is captured by the MOAPIRD's parameters (α, λ, θ).

3.2 Comparative Analysis by Performance Metrics on the Standard Deviation Chart

Table 6: Performance metrics on Standard Deviation ($\alpha=0.5, \lambda=3.0, \theta=2.1$)

n	SHEWART			IRD			MOAPIRD		
	CLI	ARL	SDRL	CLI	ARL	SDRL	CLI	ARL	SDRL
2	7.8962	14.2857	0.2607	16.4619	8.3333	0.3269	26.8366	50	0.1772
3	7.1394	12.5000	0.2744	26.0611	9.0909	0.3140	41.5379	∞	0.0000
4	5.9683	9.0909	0.3140	32.4012	10.0000	0.3010	42.8539	∞	0.0000
5	5.5381	11.1111	0.2879	36.9202	33.3333	0.1977	46.0299	∞	0.0000
6	5.0049	10.0000	0.3010	36.1156	50.0000	0.1772	44.6206	∞	0.0000
7	5.0689	11.1111	0.2879	42.6795	33.3333	0.1977	46.8470	∞	0.0000
8	4.9843	10.0000	0.3010	47.8403	50.0000	0.1772	49.2457	∞	0.0000
9	4.5892	10.0000	0.3010	48.8486	100.0000	0.1505	49.5705	∞	0.0000
10	4.8067	8.3333	0.3269	56.7641	50.0000	0.1772	55.3201	∞	0.0000

For ARL= ∞ , this reflects zero false alarms under the simulated conditions.

Table 7: Performance metrics on Standard Deviation ($\alpha=1.2, \lambda=2.2, \theta=0.4$)

n	SHEWART			IRD			MOAPIRD		
	CLI	ARL	SDRL	CLI	ARL	SDRL	CLI	ARL	SDRL
2	3.7217	14.2857	0.2607	5.3258	11.1111	0.2879	12.6623	33.3333	0.1977
3	3.3649	14.2857	0.2607	8.4317	16.6667	0.2464	19.6361	∞	0.0000
4	2.8136	9.0909	0.3140	10.5039	100.0000	0.1505	20.2573	∞	0.0000
5	2.6113	11.1111	0.2879	11.9757	∞	0.0000	21.7268	∞	0.0000
6	2.3599	10.0000	0.3010	11.7156	∞	0.0000	21.0466	∞	0.0000
7	2.3897	11.1111	0.2879	13.8400	∞	0.0000	21.9880	∞	0.0000
8	2.3491	10.0000	0.3010	15.5047	∞	0.0000	23.1553	∞	0.0000
9	2.1629	10.0000	0.3010	15.8318	∞	0.0000	23.3290	∞	0.0000
10	2.2646	8.3333	0.3269	18.3882	∞	0.0000	26.6705	∞	0.0000

For ARL= ∞ , this reflects zero false alarms under the simulated conditions.

Table 8: Performance metrics on Standard Deviation ($\alpha=1.6, \lambda=0.2, \theta=3.1$)

n	SHEWART			IRD			MOAPIRD		
	CLI	ARL	SDRL	CLI	ARL	SDRL	CLI	ARL	SDRL
2	3.1064	14.2857	0.2607	4.1066	11.1111	0.2879	10.1748	100	0.1505
3	2.8080	12.5000	0.2744	6.5445	16.6667	0.2464	15.7773	∞	0.0000
4	2.3380	8.3333	0.3269	7.8724	100.0000	0.1505	16.1551	∞	0.0000
5	2.1617	11.1111	0.2879	8.8345	∞	0.0000	17.4948	∞	0.0000
6	1.9529	10.0000	0.3010	8.6568	∞	0.0000	17.0922	∞	0.0000
7	1.9811	9.0909	0.3140	10.2411	∞	0.0000	18.1204	∞	0.0000
8	1.9575	10.0000	0.3010	11.5564	∞	0.0000	19.1601	∞	0.0000
9	1.8015	10.0000	0.3010	11.7775	∞	0.0000	19.6753	100	0.1505
10	1.8992	6.6667	0.3654	13.7876	∞	0.0000	22.0439	∞	0.0000

For ARL= ∞ , this reflects zero false alarms under the simulated conditions.

Table 9: Performance metrics on Standard Deviation ($\alpha=1.8, \lambda=0.5, \theta=1.5$)

n	SHEWART			IRD			MOAPIRD		
	CLI	ARL	SDRL	CLI	ARL	SDRL	CLI	ARL	SDRL
2	3.6374	14.2857	0.2607	5.1318	11.1111	0.2879	11.9797	50.0000	0.1772
3	3.2901	12.5000	0.2744	8.1113	14.2857	0.2607	18.6832	∞	0.0000
4	2.7450	8.3333	0.3269	9.9672	50.0000	0.1772	19.2972	∞	0.0000
5	2.5430	11.1111	0.2879	11.3159	∞	0.0000	20.8525	∞	0.0000
6	2.2974	10.0000	0.3010	11.0635	∞	0.0000	20.4073	∞	0.0000
7	2.3300	10.0000	0.3010	13.1102	∞	0.0000	21.5565	∞	0.0000
8	2.2974	10.0000	0.3010	14.7619	∞	0.0000	22.7216	∞	0.0000
9	2.1150	10.0000	0.3010	15.0721	∞	0.0000	23.0263	∞	0.0000
10	2.2224	7.1429	0.3525	17.5870	∞	0.0000	25.8349	∞	0.0000

For ARL= ∞ , this reflects zero false alarms under the simulated conditions.

Table 10: Metrics and remarks for Standard Deviation Chart

Metric	Shewhart Chart	IRD Chart	MOAPIRD Chart (Proposed)	Remark
False Alarms (ARL)	Very High (6.67-14.29)	Low to Zero (8.33- ∞)	Zero to Very Low (33.33- ∞ , mostly ∞)	MOAPIRD eliminates false alarms. IRD improves with larger samples. Shewhart shows high false alarm rates
Run Length Variability (SDRL)	High (0.261-0.365)	Zero to Moderate (0-0.327)	Zero to Low (0-0.198, mostly 0)	MOAPIRD is highly predictable. IRD is moderately variable. Shewhart is unpredictable.
Sensitivity (CLI)	Too Sensitive (1.80-7.90, narrow)	Moderate to Wide (4.11-56.76)	Optimally Balanced (10.17-55.32)	MOAPIRD offers optimal, balanced limits. IRD's limits are acceptable but vary. Shewhart's limits are too narrow.
Sample Size Robustness	Poor with degradation at larger n	Good adaptation with improvement as n increases	Excellent stability across all n	MOAPIRD is stable across all sample sizes. IRD improves with larger samples. Shewhart degrades with larger samples.
Parameter Robustness	Consistently poor across all configurations	Good with configuration-dependent performance	Excellent consistency across all parameter sets	MOAPIRD is consistently excellent. IRD is parameter sensitive. Shewhart performs poorly.
Practical Reliability	Predictably inadequate	Good but inconsistent at small n	Consistently excellent	MOAPIRD is reliable. IRD exhibits provisional reliability.

The examination of standard deviation charts substantiates that MOAPIRD persists as the superior and most robust method, exhibiting remarkable and consistent performance across all conditions, characterized by near-optimal accuracy, negligible false alarms, and well-balanced control limits. The IRD method shows a marked improvement for larger sample sizes ($n \geq 5$) but remains inconsistent and prone to false alarms in the context of smaller samples. Conversely, the Shewhart chart continues to demonstrate poor performance, marked by low accuracy and unacceptably high false alarm rates, further entrenching its inadequacy for effective quality control applications aimed at monitoring process variation.

3.3 Real Data Application

A validation study with real-world data is provided here to validate the simulation results of the MOAPIRD-based S-chart. This study focuses on the quality control of engine oils, where engineers measure the percentage increase in viscosity (PVIS). Reference oil, Ref Oil 434, was analyzed to establish a quality standard. As detailed in Table 11, a dataset from Almulhim et al. (2024) comprising 500 measurements, grouped into 50 subgroups, was analyzed using the proposed diagram to determine whether the viscosity profile of Ref Oil 434 deviated from the control parameters of the standard production process.

Table 11: Data for PVIS of Ref Oil 434

No.	X ₁	X ₂	X ₃	X ₄	X ₅	X ₆	X ₇	X ₈	X ₉	X ₁₀
1	54.2	103.7	160.7	381.5	108.4	870.8	114.1	120.6	67.4	185.7
2	90.7	411.3	160.7	106.5	114.1	114.1	69.2	106.3	119.1	133
3	106.5	83.7	107.4	92.2	104	110.9	69.2	35.4	297.9	73.9
4	297.9	89.9	35.4	76.1	252.2	54.2	155.1	381.5	373.1	94.2
5	108.4	613.6	137.6	76.1	110.8	411.3	169	83.7	373.1	110.8
6	110.9	356	54.2	107.4	83.7	494.5	151.9	196.5	303.3	185.7
7	307.6	88.6	97.8	94.2	101.5	129.6	76.1	90.8	106.5	103.4
8	119.1	93	145.9	667.9	76.9	94.9	80.7	356	141.2	75.5
9	83.5	127.6	93	83.5	72.3	82.8	53.2	83.1	85	86.8
10	108.9	66.4	300.5	134	115.4	117.5	103.7	103.7	83.1	300.5
11	76.1	133.3	303.3	89.9	185.7	373.1	70	80.7	60.9	69.2
12	94.2	252.2	114.1	103.7	106.5	99.2	122.7	75.5	127.6	133.3
13	105.8	101.5	53.2	70	151.9	89.9	160.7	196.5	97.1	249.5
14	88.9	73.9	151.9	151.3	307.6	303.3	356	300.5	46.2	107.4
15	104	205	90.8	667.9	83.1	307.6	252.2	88.9	613.6	106.3
16	613.6	101.5	53.6	117.5	303.6	81.6	94.2	106.3	97.1	110.2
17	185.7	90.8	119.1	324.4	74.8	86.7	108.4	90.7	324.4	205
18	146.3	105.8	90.8	115.4	62.8	160.7	107.4	303.3	83.1	83.5
19	97.8	46.2	667.9	185.7	83.1	83.5	80.7	160.7	124.8	155.1
20	97.1	141.2	76.1	169	151.9	494.5	70	94.2	92.2	83.1
21	129.6	88.9	411.3	90.7	151.9	137.6	226.3	106.5	307.6	94.8
22	66.4	281.6	86.8	179.1	124.8	94.9	83.1	118.9	93.7	103.7
23	160.7	83.5	92.2	105.8	146.3	300.5	151.9	494.5	124.8	86.8
24	80.7	117.5	411.3	179.1	120.6	137.6	76.1	196.5	145.9	88.9
25	93.7	134	185.7	870.8	69.2	307.6	67.4	76.1	185.7	76.1
26	89.9	80.7	97.1	145.9	81.6	119.1	145.9	118.9	76.1	85
27	90.8	115.4	97.1	92.2	83.5	88.6	94.2	133.3	82.8	205
28	99.2	70	281.6	60.9	70	147.2	99.2	303.6	55.4	114.1
29	226.3	107.2	226.3	76.9	297.9	70	106.3	303.6	97.8	107.2
30	226.3	46.2	83.1	93.7	35.4	185.7	870.8	83.5	90.8	110.2
31	179.1	373.1	300.5	300.5	114.1	53.6	106.3	122.7	356	101.5
32	108.9	108.1	83.7	155.1	185.7	373.1	147.2	94.8	88.8	107.4
33	72.3	53.2	46.2	137.6	124.8	179.1	69.7	76.1	89.9	97.8
34	72.3	86.8	60.9	107.2	117.5	94.8	76.1	94.9	53.2	160.7
35	307	89.9	151.3	373.1	46.2	70	281.6	104	86.8	90.8
36	67.4	88.8	83.7	54.2	196.5	127.6	373.1	69.7	70	61.1
37	133	115.4	667.9	172	94.9	124.8	107.4	85.9	108.4	185.7
38	88.6	127.6	110.2	103.7	147.2	147.2	303.3	72.3	86.7	303.6
39	300.5	108.4	110.8	115.4	92.2	141.2	103.7	119.1	88.8	93.7
40	613.6	97.1	134	97.8	205	103.4	108.4	108.1	103.7	110.2

41	93	90.8	297.9	110.2	124.8	151.9	870.8	179.1	252.2	85
42	137.6	356	80.7	106.3	75.5	179.1	118.9	82.8	120.6	411.3
43	46.2	381.5	62.8	411.3	81.6	86.7	88.8	108.9	90.7	97.1
44	128.7	76.1	108.9	160.7	99.2	110.2	72.3	62.8	97.8	53.6
45	73.9	81.6	107.2	103.7	85.9	35.4	117.5	151.3	90.7	133.3
46	90.7	101.5	297.9	85.9	107.2	667.9	148.2	108.1	97.1	373.1
47	494.5	103.7	196.5	146.3	160.7	134	53.2	119.1	133	94.6
48	297.9	99.2	133.3	103.7	101.5	97.8	494.5	249.5	129.6	103.4
49	83.1	46.2	103.7	110.9	86.7	35.4	103.7	226.3	169	146.3
50	105.8	69.7	108.4	196.5	303.3	86.7	411.3	75.5	249.5	110.8

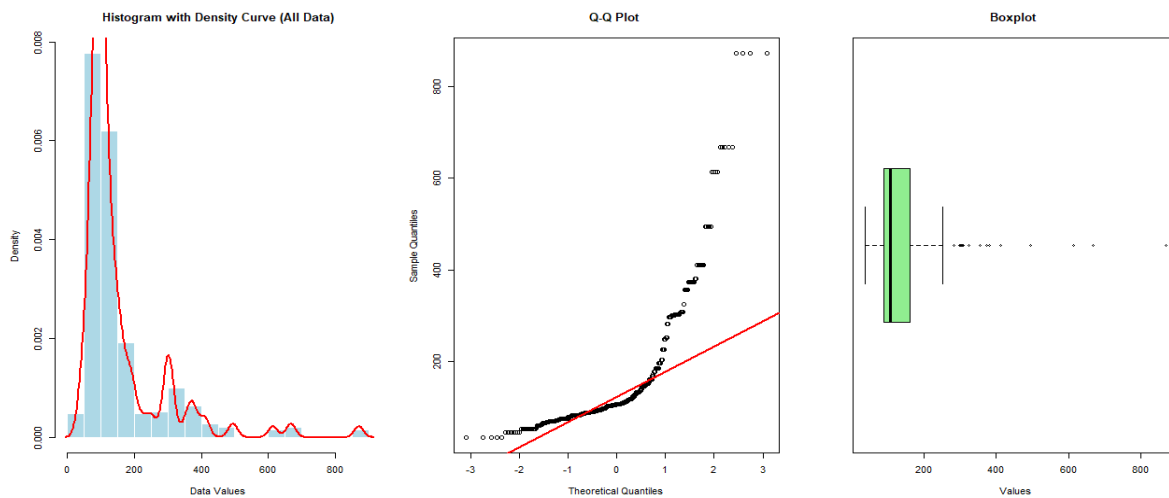


Figure 1: plots of Density, Q-Q, and Boxplot of the PVIS data for Ref Oil 434

Table 12: Summary statistics

Count	Mean	SD	Mini	Q1	Q2	Q3	Max	Skew	Kut
500	154.75	128.98	35.4	86.8	107.2	160.7	870.8	2.83	9.68

The density and Q-Q plots of the data, as illustrated in Figure 1, are used to help figure out the shape of the data distribution of PVIS of is 2.817. The findings indicate that the data is not distributed evenly, and there exists indications that the data belongs to a positively skewed distribution. With the fact that the data are

Ref Oil 434 (Table 11). The Jarque Bera Test of normality is also 2570.2, and the p-value is $2.2e^{-16}$. In addition, the data skewness coefficient is skewed, it is necessary to apply the non-normal method in constructing the control limits

that will not give false alarms. The data was modeled using MOAPIRD, and the graphical representation is given in Figure 2. Hence, it is evident that the statistics are also approximately a Marshall-Olkin Alpha Power Inverse Rayleigh random variable.

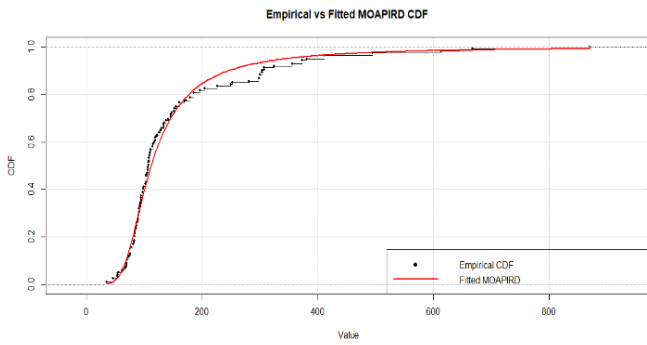


Figure 2: The CDF for Reference Oil 434's PVIS data vs. Hypothetical MOAPIRD.

The \bar{S} of the PVIS for Ref Oil 434 data were calculated and used to develop control limits for the proposed charts at $\alpha = 1.8$, $\lambda = 0.5$, $\theta = 1.5$. Figure 3 shows the respective control charts

Shewhart S-Chart: $UCL = B_4\bar{S}$, $CL = \bar{S}$ and $LCL = B_3\bar{S}$ (11)

IRD S-chart: $UCL = B^{**}_3\bar{S}$, $CL = \bar{S}$ and $LCL = B^*_3\bar{S}$ (12)

MOAPIRD S-Chart: $UCL = B^{**}_{3p}\bar{S}$, $CL = \bar{S}$ and $LCL = B^*_{3p}\bar{S}$ (13)

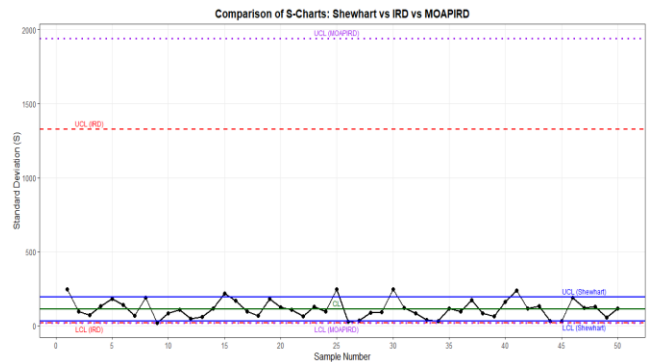


Figure 3: S-Charts for Shewhart, IRD, and MOAPIRD for Thickness of Oil Seal data

Figure 3 demonstrates that the Shewhart S-chart produces comparatively small control limits, thus generating more out-of-control signals, especially in periods 2, 4, 6, 24, 30, 41, and 46, where the extreme data points have exerted an effect on the sub-group variability. Such a phenomenon implies that there is an inflated type 1 error, which assumes normality that underlies the Shewhart chart. However, the S-charts created based on the IRD and MOAPIRD approaches provide much broader and more sufficient control limits, with the values of most of them being in the control range, which suggests higher resistance to asymmetry and skewed distributions. One can mention the fact that the MOAPIRD S-chart demonstrates the highest level of stability and broader control limits in comparison with IRD. The extended upper control limit set by MOAPIRD minimizes the possibility of Type I errors, hence, guarding against false alarms due to the misinterpretation

of natural causes of variation in processes as assignable causes, which confirms its better usage in the monitoring of process variability in a non-normal industrial situation. This comparison points out the strength of the MOAPIRD-based methodology in working with data of non-normally distributed processes, and thus in the establishment of corrective measures that are motivated not necessarily by the variation that is inherent to the PVIS measurements of the reference oil 434.

4.0 CONCLUSION

This study applies to the Standard Deviation (S) control chart that is built on the Marshall-Olkins Alpha Power Inverse Rayleigh Distribution (MOAPIRD) to track process variability in a non-normal environment. According to the theoretical derivations and the findings of the simulations, it can be concluded that the proposed chart is more useful than the classical S-chart with reference to the Shewart and Inverse Rayleigh distribution in terms of identifying the variability changes. S-chart, as adopted in the MOAPIRD, is more sensitive and reliable in the case of positively skewed and heavy-tailed datasets, and this makes it a very important component in the quality control of a situation in an industrial setting. The technique used in making Shewhart-type S-control charts to monitor non-normal distribution can be applied to other control chart techniques, which include Exponential Weighted Moving Average (EWMA), Cumulative Sum (CUSUM), and attribute control charts. Moreover, the distribution may be used in process capability

research and acceptance sampling methods, and its usefulness may be explored in other fields like reliability research, survival research, hydrology research, and studies related to health.

Data Availability Statement

This study utilizes the dataset from Almulhim et al. (2024), with R codes for creating all charts and graphs accessible through the corresponding author by reasonable request.

Conflicts of Interest Statement

The authors do not declare any conflicts of interest.

Acknowledgement

The authors used ChatGPT (OpenAI) and Claude (OpenAI) for the development of R codes, as well as the SciSpace AI writing tool. All contents were reviewed, refined, and verified by the authors.

Supporting Information:

Tables 1 to 9 and figures 1 to 3 are the authors' computations with the aid of R codes.

REFERENCES

- Aako, O. L., Adekeye, K. S., Adewara, J. A., & Nkemnole, E. B. (2020). X bar and R control charts based on Marshall-Olkin inverse log-logistic distribution for positive skewed data. *African Journal of Pure and Applied Sciences*, 1(1), 9–16. <https://doi.org/10.33886/ajpas.v1i1.167>.
- Aako, O. L., Adekeye, K. S., & Adewara, J. A. (2024). A standard deviation control chart for

- the Marshall–Olkin inverse log-logistic distribution. *African Journal of Pure and Applied Sciences*, 5(1), 118–123.
- Abu-Shawiesh, M.O.A. (2008). A Simple Robust Control Chart Based on MAD. *Journal of Mathematics and Statistics*, 4(2), 102-107.
- Adegbite, I.O., Adekeye, K.S., & Aako, O.L. (2024). Marshall-Olkin Alpha Power Inverse Rayleigh Distribution: Properties, estimation and applications. *Reliability: Theory & Applications*, 19(1 (77)), 564–576.
- Adekeye, K. S., & Azubuikwe, P. I. (2012). Derivation of the limits for control chart using the median absolute deviation for monitoring non-normal process. *Journal of Mathematics and Statistics*, 8(1), 37-41.
- Adewara, J. A., & Aako, O. L. (2018). Variable control charts based on percentiles of exponentiated Lomax distribution. *Nigerian Journal of Pure and Applied Sciences*, 31(2), 3265-3271.
- Adewara, J. A., Adekeye, K. S., & Aako, O. L. (2020). On performance of Gompertz-based control charts. *Journal of Probability and Statistics*, 2020(5), 1-9. <https://doi.org/10.1155/2020/8820652>.
- Almulhim, F. A., Malik, S., Hanif, M., Hassaballa, A. A., Nabi, M., & Usman, A. M. (2024). Joint monitoring of mean and variance using Max-EWMA control chart under Lognormal process with application to engine oil data. *Scientific Reports*, 14(1), 13811. <https://doi.org/10.1038/s41598-024-64077-6>.
- Atta, A. M. A., Yahaya, S. S. S., Zain, Z., & Ahmad, N. (2020). New skewness correction S control chart for monitoring dispersion of skewed data with application in healthcare. *Systematic Reviews in Pharmacy*, 11(4), 217–222.
- Chan, L. K., & Cui, H. J. (2003). Skewness correction X and R charts for skewed distributions. *Naval Research Logistics*, 50(1), 1-19. <https://doi.org/10.1002/nav.10046>.
- Chang, Y. S., & Bai, D. S. (2001). Control charts for positively-skewed populations with weighted standard deviations. *Quality and Reliability Engineering International*, 17(5), 397-406. <https://doi.org/10.1002/qre.416>.
- Chen, W. (1996). The effects of SPC on the target of process quality improvement. *Journal of Quality Technology*, 28(2), 224-232.
- Chou, C. Y., Li, M. H. C., & Wang, P. H. (2001). Economic statistical design of averages control charts for monitoring a process under non-normality. *The International Journal of Advanced Manufacturing Technology*, 17(8), 603–609. <https://doi.org/10.1007/s001700170154>.
- Malik, A. S., & Ahmad, S. P. (2018). A new inverse Rayleigh distribution: Properties and monitoring of process location and dispersion. *Measurement and Control*, 55(5-6), 370–384. <https://doi.org/10.1177/00202940211043085>.
- Montgomery, D. C. (2013). Introduction to statistical quality control (7th ed.). Wiley.
- Oladipupo, O.O., Adekeye, K.S., Olaomi, J.O., & Alayande, S.A. (2025). Improved non-parametric double homogenously weighted moving average control chart for monitoring changes in process location. *Statistics, Optimization & Information Computing*, 14(5), 2118–2130. <https://doi.org/10.19139/soic-2310-5070-2244>.
- Panda, S. & Wang, M. (2025). Bootstrap-Based Control Chart for Percentiles of the Generalized Lognormal Distribution With Reliability Applications. *Quality and Reliability Engineering International*. <https://doi.org/10.1002/qre.3722>.
- Rosaiah, K., Boyapati, S. R. & Jyothi, P. (2021). Variable control charts based on percentiles of the new Rayleigh-Pareto distribution. *International Journal of Statistics and Applied Mathematics*. 6(3), 122-131. <https://doi.org/10.22271/math.2021.v6.i3b.694>.
- Shibo, X., Yali, W., & Wenqing, L. V. (2014). Standard deviation control chart based on weighted standard deviation method. *Proceedings of the 33rd Chinese Control Conference* (pp. 6192-6196). July 28-30, Nanjing, China.
- Srinivasa R, B., & Kantam, R. R. L. (2012). Mean and range charts for skewed distributions: a comparison based on a half-logistic distribution. *Pakistan Journal of Statistics*, 28(4), 437-444.
- Wan, Q., & Zhu, M. (2022). Optimal design of an improved X and R control chart for joint monitoring of process location and dispersion. *Measurement and Control*, 55(5-6), 370–384. <https://doi.org/10.1177/00202940211043085>.
- Ying-Chin H., Shih-Chou K., & Chih-Feng C. (2021). Robustness of dispersion control charts in skewed distributions. *International Journal of Industrial Engineering*, 28(4), 372–389.